Eur J Nucl Med Mol Imaging. Author manuscript; available in PMC 2013 June 24.

Published in final edited form as:
Eur J Nucl Med Mol Imaging. 2010 May ; 37(5): 942–953. doi:10.1007/s00259-009-1332-5.

Dose-response assessment of tariquidar and elacridar and regional quantification of P-glycoprotein inhibition at the rat blood-brain barrier using (*R*)-[^{11}C]verapamil PET

Claudia Kuntner[1,*], **Jens P. Bankstahl**[2], **Marion Bankstahl**[2], **Johann Stanek**[3], **Thomas Wanek**[1], **Gloria Stundner**[1], **Rudolf Karch**[4], **Rebecca Brauner**[5], **Martin Meier**[6], **Xiaoqi Ding**[7], **Markus Müller**[3], **Wolfgang Löscher**[2], and **Oliver Langer**[1,3]

[1]Molecular Medicine, AIT Austrian Institute of Technology GmbH, Seibersdorf, Austria

[2]Department of Pharmacology, Toxicology & Pharmacy, University of Veterinary Medicine Hannover, Germany

[3]Department of Clinical Pharmacology, Medical University of Vienna, Austria

[4]Department of Medical Computer Sciences, Medical University of Vienna, Austria

[5]Chemical Analytics, Seibersdorf Labor GmbH, Seibersdorf, Austria

[6]Department of Cardiology and Angiology, Hannover Medical School, Germany.

[7]Institute of Diagnostic and Interventional Neuroradiology, Hannover Medical School, Germany

Abstract

Purpose—Overactivity of the multidrug efflux transporter P-glycoprotein (P-gp) at the blood-brain barrier (BBB) is believed to play an important role in resistance to central nervous system drug treatment. (*R*)-[^{11}C]verapamil (VPM) PET can be used to measure the function of P-gp at the BBB, but low brain uptake of VPM hampers the mapping of regional differences in cerebral P-gp function and expression. The aim of this study was to evaluate the dose-response relationship of two potent P-gp inhibitors and to investigate if increased brain uptake of VPM mediated by P-gp inhibition can be used to assess regional differences in P-gp activity.

Methods—Two groups of Sprague-Dawley rats (n=12) underwent single VPM PET scans at 120 min after administration of different doses of the P-gp inhibitors tariquidar and elacridar. In an additional 6 rats, paired VPM PET scans were performed before and after administration of 3 mg/kg tariquidar.

Results—Inhibitor administration resulted in an up to 11-fold increase in VPM brain distribution volumes (DV) with ED_{50} values of 3.0±0.2 and 1.2±0.1 mg/kg for tariquidar and elacridar, respectively. In paired PET scans, 3 mg/kg tariquidar resulted in regionally different enhancement of brain activity distribution, with lowest DV in cerebellum and highest DV in thalamus.

Conclusion—Our data show that tariquidar and elacridar are able to increase VPM brain distribution in rat brain up to 11-fold over baseline at maximum effective doses, with elacridar being about 3 times more potent than tariquidar. Regional differences in tariquidar-induced modulation of VPM brain uptake point to regional differences in cerebral P-gp function and expression in rat brain.

[*]Corresponding author: Claudia Kuntner, PhD, Molecular Medicine, AIT Austrian Institute of Technology GmbH, 2444 Seibersdorf, Austria, Tel.: +43 50 550 3471. Fax: +43 50 550 3473. claudia.kuntner@ait.ac.at.
Claudia Kuntner and Jens P. Bankstahl contributed equally to this study.

Europe PMC Funders Author Manuscripts

Keywords

small animal PET; (*R*)–[^{11}C]verapamil; tariquidar; elacridar; P-glycoprotein, blood-brain barrier, regional

Introduction

The adenosine binding cassette (ABC) efflux transporter P-glycoprotein (P-gp, ABCB1) is highly expressed in the luminal membrane of brain capillary endothelial cells which are a constitutive component of the blood-brain barrier (BBB), thereby limiting brain entry of many xenobiotic compounds like drugs or toxins. Regional overactivity of P-gp and related transporters in the BBB is believed to contribute to the phenomenon of drug resistance in neurological disorders, such as epilepsy and depression, by impeding therapeutically effective concentrations of central nervous system (CNS) drugs at their sites of action [1].

Positron emission tomography (PET) with the radiolabelled P-gp substrate (*R*)-[^{11}C]verapamil (VPM) is an innovative method of measuring P-gp function at the BBB [2]. Studies employing pharmacological P-gp inhibition in rats have shown that the brain distribution volume (*DV*) of VPM is inversely related to cerebral P-gp activity [3, 4].

So far, most studies using VPM PET to explore regional differences in cerebral P-gp activity in different patient groups have failed to detect pronounced regional differences in VPM *DV*s [5, 6]. This is most likely related to the fact that the high-affinity P-gp substrate VPM is very effectively kept out of brain parenchyma by P-gp mediated efflux. The resultant low brain uptake of VPM and its radiolabelled metabolites appears to be largely independent of regional differences in P-gp function and expression. A promising strategy to increase brain uptake of VPM and thereby facilitate the mapping of regional differences in cerebral P-gp function and expression is to perform VPM PET scans after P-gp modulation with P-gp inhibiting drugs. It has been shown, both in animals and humans, that the P-gp inhibitors cyclosporine A, valspodar and tariquidar are able to enhance brain uptake of VPM [3, 7-9]. However, prior to using P-gp inhibiting drugs in combination with VPM PET scans, a detailed understanding of their dose-response relationships is mandatory because low inhibitor doses will possibly have no impact on brain uptake of VPM whereas high doses might completely inhibit the P-gp pump and result in P-gp independent brain uptake of VPM.

The aim of this study was to examine the effect of different doses of the third-generation P-gp inhibitors tariquidar and elacridar on brain uptake, peripheral metabolism and plasma protein binding of VPM in rats. An optimised inhibitor dose of tariquidar was then used in a paired scan paradigm consisting of a baseline VPM scan and a second scan after inhibitor administration for the mapping of regional differences in P-gp function and expression in rat brain.

Materials and methods

Animals

Adult female Sprague-Dawley rats (Harlan Nederland, Horst, Netherlands) weighing 220-250 g were used for this study. Animals were kept under controlled environmental conditions (22±1°C; 40–70% humidity; 12-h light/dark cycle) with free access to standard laboratory animal diet and tap water. Before being used in the experiments, the rats were allowed to adapt to the new conditions for ≥1 week. The study was approved by the local Animal Welfare Committee and all study procedures were performed in accordance with the

Europe PMC Funders Author Manuscripts

Austrian Animal Experiments Act. All efforts were made to minimize pain or discomfort as well as the number of animals.

Prior to each experiment, the animals were placed in a chamber containing 2% isoflurane in oxygen. When unconscious, the animals were taken from the chamber and kept under anaesthesia with 1.8 to 0.6% isoflurane administered *via* a mask during the whole experiment. During the 240 min imaging period the isoflurane level was adjusted depending on depth of anaesthesia. Animal monitoring was performed visually by assessment of breathing rate and perfusion of acra, as well as by testing reflexes. A humidifier was used to moisten the gas mixture before supplying it to the animal, thus preventing impairment of air passages. Femoral artery and femoral vein were cannulated to allow repeated arterial blood sampling as well as intravenous administration of tariquidar, elacridar and VPM. After surgery, animals were positioned in the imaging chamber (T8328 animal cradle from Bruker BioSpin MRI) of the microPET scanner, which was kept at 38°C throughout the whole experiment. A stereotactic holder attached to the bed, consisting of ear plugs and a tooth bar, was used to fixate the animal's head to ensure a reproducible position during the PET studies.

For magnetic resonance imaging (MRI) anaesthesia was induced by a mixture of air and 3% isoflurane. During MRI, animals were anaesthetised with 1.0–1.5% isoflurane/O_2 *via* a nose cone with monitoring of respiratory rate.

Chemicals

Unless otherwise stated, all chemicals were of analytical grade and obtained from Sigma-Aldrich Chemie GmbH (Schnelldorf, Germany) or Merck (Darmstadt, Germany). Isoflurane was obtained from Baxter VertriebsGmbH (Vienna, Austria). Tariquidar dimesylate was obtained from Xenova Ltd. (Slough, Berkshire, UK) and elacridar hydrochloride was obtained from GlaxoSmithKline (Research Triangle Park, NC, USA). For administration, tariquidar was freshly dissolved on each experimental day in 2.5% (g/v) aqueous dextrose solution and injected intravenously (i.v.) at a volume of 3 ml/kg over 1 min. Elacridar was dissolved in 20% (v/v) aqueous ethanol and injected i.v. at a volume of 4 ml/kg over 1 min. Enantiomerically pure VPM was synthesised from (*R*)-norverapamil and [^{11}C]methyl triflate as described earlier [10].

PET experimental procedure

A microPET Focus220 scanner (Siemens, Medical Solutions) was used for the experiment. It has 168 detector modules providing a 7.6 cm axial and 22 cm transaxial field of view. Reconstructed image resolution (filtered back projection) is 1.3 mm (full width at half maximum) in the central field of view and remains under 2 mm within the central 5 cm diameter field of view [11]. Anaesthetised animals were positioned in the imaging chamber and VPM (77±18 MBq, 0.55±0.13 nmol, n=44) dissolved in 0.3±0.1 ml of phosphate-buffered saline (pH=7.4)/ethanol (9/1, v/v) was administered as an i.v. bolus *via* the femoral vein over 29±5 s. The injected activity amount was still within the linear range of the PET scanner [11]. At the start of radiotracer injection dynamic PET imaging was initiated. List mode data were acquired for the defined time period with an energy window of 350-750 keV and 6 ns timing window. Before each PET scan, a transmission scan using a Co-57 point source was recorded over 10 min.

During the first 3 min after radiotracer injection, 2-μl arterial blood samples were continuously withdrawn using pre-weighted micropipettes followed by further 10-μl samples taken at 5, 10, 20, 30, 40, 50 and 60 min after injection. Moreover, one blood sample (0.6 ml) was collected into a heparinised vial at 20 min after tracer injection in order

to determine metabolism of VPM (see below). The 20 min blood sample was also used to measure the ratio of plasma to whole-blood activity. Radioactivity in the blood samples was measured in a 1-detector Wallac gamma counter (Perkin Elmer Instruments, Wellesley, MA, USA), which was cross-calibrated with the PET camera. The removed blood volume was substituted by the same volume of 0.9% (w/v) aqueous saline solution containing 20 IE/ml sodium heparin to prevent clotting of catheters. Blood radioactivity data were corrected for radioactive decay and expressed as percent injected dose per gram blood (%ID/g).

For PET imaging, animals were divided into 3 groups. The first group was used for the dose-response assessment of tariquidar and elacridar. In these animals, single 60 min dynamic PET scans were recorded 120 min after i.v. administration of inhibitors. The time point of 120 min was chosen as plasma levels of inhibitor can be expected to have stabilised (i.e. remained constant for the duration of the PET scan) at this time point. Tariquidar was administered at doses of 30, 15, 7.5, 3.75, 2.6 and 1.5 mg/kg (each with n=2). Elacridar was injected at doses of 7.5 (n=2), 5 (n=3), 2 (n=2), 1 (n=3) and 0.3 mg/kg (n=2), respectively.

In the second group, the time course of P-gp inhibition by tariquidar and elacridar was monitored. These animals underwent single 240 min dynamic PET scans, during which inhibitor (tariquidar, 15 mg/kg or elacridar, 5 mg/kg, n=2 per inhibitor) was injected over approximately 1 min at 60 min after radiotracer injection.

In the third group (n=6), paired VPM PET scans were performed. A dynamic 60 min baseline PET scan (scan 1) was followed by administration of 3 mg/kg tariquidar and a second 60 min PET scan at 120 min after tariquidar administration (scan 2).

At the end of the last PET scan the animals were sacrificed. A terminal blood sample (5 ml) was collected and centrifuged to obtain plasma and whole brains were removed. An aliquot of the plasma sample (groups 1 and 3) was used to assess metabolism of VPM (see below). Brains and the remainder of plasma were stored at −20°C until measurement of tariquidar or elacridar concentrations using a previously described combined liquid chromatography tandem mass spectrometry (LC/MS) assay [9].

Magnetic resonance imaging (MRI)

One naïve age-matched female Sprague-Dawley rat, which was not examined by PET scanning, underwent MRI for co-registration with PET images (see below). MRI was conducted on a 7 Tesla animal scanner (Pharmascan 70/16, Bruker BioSpin MRI Ettlingen) by using a T2-weighted MSME sequence with a 5500 ms repetition time and 35 ms echo time. Coronal sections with a field of view of 3.5 × 3.5 cm were acquired. In order to provide detailed anatomical structure a slice thickness of 0.8 mm was used. The animal was placed in a prone position and fitted with a tooth bar and head holder in the same cradle as used for the PET scans. Images were acquired using a 38 mm volume coil (T10327V3) serving simultaneously as transmitter and receiver coil.

Metabolism and plasma protein binding of VPM

In a group of 6 rats VPM was injected without performing PET examination in order to assess the percentage of unchanged parent, including its lipophilic [^{11}C]metabolites which are also P-gp substrates [2, 12], in plasma at 10, 20, 30, 40 and 60 min after radiotracer injection using a previously described solid-phase extraction assay [13, 14]. Correction of activity counts in plasma for lipophilic [^{11}C]metabolites was not performed as this would have required high-performance liquid chromatography (HPLC) analysis, which was not feasible due to the small amounts of blood available from individual rats resulting in low activity count rates. Additionally, VPM metabolism during PET scanning of groups 1 and 3 was studied in plasma at 20 and 60 min after tracer injection (60 min sample corresponded

to the terminal sample and was not obtained for the first scan in group 3). Plasma protein binding of VPM was determined by incubating plasma samples (500 μl) obtained from naïve animals as well as from animals which had received inhibitor with VPM dissolved in physiological saline/ethanol (9/1) (about 0.4 MBq, 5 μl) for 20 min at 37°C. Aliquots of the incubation solution (200 μl) were then transferred into the sample reservoir of Amicon Microcon YM-10 centrifugal filter devices (Millipore Corporation, USA), which had been pre-washed with unlabelled racemic verapamil dissolved in water (10 mg/ml, 100 μl) to block non-specific binding of the radiotracer to the filter membrane. The centrifugal filter devices were then centrifuged for 30 min at 12000×g (25°C) using a Heraeus Fresco 17 centrifuge (Thermo Electron Corporation, Waltham, USA). Sample reservoirs and ultrafiltrates were then measured for radioactivity in a gamma counter, corrected for radioactive decay and percent protein binding of VPM expressed as percentage of radioactivity in the sample reservoir relative to total radioactivity.

PET data analysis

The PET data from the 60 min dynamic scans were sorted into 3-dimensional sinograms according to the following frame sequence: 8 × 5 s, 2 × 10 s, 2 × 30 s, 3 × 60 s, 2 × 150 s, 2 × 300 s and 4 × 600 s. For the 240 min scans (used to monitor the time course of P-gp modulation) the following frame sequence was used: 8 × 5 s, 2 × 10 s, 2 × 30 s, 3 × 60 s, 2 × 150 s, 2 × 300 s, 4 × 600 s, 5 × 120 s, 5 × 600 s and 6 × 1200 s. PET images were reconstructed by Fourier rebinning of the 3-D sinograms followed by 2-dimensional filtered back projection with a ramp filter resulting in a voxel size of 0.6 × 0.6 × 0.8 mm^3. The standard data correction protocol (normalisation, attenuation and decay correction) was applied to the data. A calibration factor for converting units of PET images into absolute radioactivity concentration units was generated by imaging a phantom filled with a known concentration of VPM. Regions of interest (ROI) for whole brain were manually outlined on multiple planes of the PET summation images (0-60 min) using the image analysis software Amide [15]. Volumes of interest (VOIs) were transferred to the PET images of the individual time frames and time-activity curves (TACs), expressed in units of kBq/ml, were calculated for each VOI. To facilitate comparison of TACs of different animals, radioactivity concentrations were dose-normalised and expressed as percent injected dose per gram tissue (%ID/g).

Images of the paired VPM PET scans before and after tariquidar administration were co-registered with magnetic resonance (MR) images of one naïve female Sprague-Dawley rat using PMOD (version 2.7.5, PMOD group, Switzerland). Six brain ROIs (frontal motor cortex, corpus striatum (caudate putamen), cerebellum, entorhinal cortex, hippocampus and thalamus) were manually outlined on multiple transverse planes in MR images. As the MR and PET images covered different body regions of the studied animal (MR images, head region only; PET, head and thorax) the PET images were resliced to achieve a high overlap and manually co-registered afterwards. As the pituitary gland exhibited a strong radioactive signal and was also well defined in the MR images, it was used as one reference point for co-registration. A rigid transformation was used, as the shape of the brain was very similar among different animals. Afterwards, the brain ROIs from the MR images were assigned to the PET images and TACs for the selected brain VOIs were extracted. ROIs were further analysed by compartment modelling.

Kinetic modelling of VPM

The input function was constructed by linear interpolation of the measured arterial blood activity data and by multiplication by the ratio of plasma to whole-blood activity, which had been determined in individual animals. The activity data for the 10, 20, 30, 40 and 60 min time points were corrected for polar [^{11}C]metabolites of VPM by multiplication by the

fraction of unchanged VPM and its lipophilic [^{11}C]metabolites, which had been determined in the group of 6 rats (see above). This approach was feasible as we had not seen any differences in VPM metabolism between inhibitor-treated and untreated rats. The lipophilic [^{11}C]metabolites of VPM were included in the input function as they can be expected to behave similarly to parent tracer because they are also P-gp substrates [2, 12]. A 2-tissue 4-rate constant (2T4K) compartment model was fitted to the VPM TACs in rat brain as described before [6, 14]. In order to obtain a model-independent estimate of the distribution volume *DV*, Logan graphical analysis was applied to the PET and arterial plasma data using MATLAB (Mathworks, Natick, MA, USA) as described before [6]. Sigmoidal curves were fitted to the *DV*s of VPM plotted against inhibitor doses or inhibitor plasma concentrations using the Hill equation included in the OriginPro 7.5G software package (OriginLab Corporation, Northampton, USA). The half-maximum effect dose ED_{50} (mg/kg), the half-maximum effect concentration EC_{50} (ng/ml), maximum effect DV_{max} (ml·ml^{-1}) and the Hill factor n were extracted from the fit.

Statistical analysis

For all calculated outcome parameters, differences between baseline scans (before inhibitor administration) and scans after inhibitor administration were tested using a two-tailed paired Student's *t*-test. Differences between *DV*s from the six brain ROIs were tested by one-way ANOVA followed by Bonferroni's multiple comparison test. The level of statistical significance was set to 5%.

Results

Mean brain TACs after administration of different doses of tariquidar and elacridar are shown in Fig. 1a and Fig. 1b, respectively. In Fig. 1c, PET summation images (horizontal plane) from the 60 min scans after administration of 1.5, 2.6, 3.75 and 15 mg/kg of tariquidar are shown. Table 1 summarises the estimated outcome parameters of the 2T4K model for baseline scans as well as for scans after administration of different inhibitor doses. Wholebrain *DV* values after administration of 1.5, 2.6, 3.75, 7.5, 15 and 30 mg/kg of tariquidar were increased by 2.2±1.1, 4.7±1.1, 7.0±1.1, 10.1±0.8, 9.9±1.8, and 10.2±0.3, respectively, as compared to baseline scans. After administration of 0.3, 1, 2, 5, and 7.5 mg/kg of elacridar, *DV*s were increased by factors of 1.0±0.6, 3.5±1.5, 9.4±1.5, 8.9±1.4, and 11.3±0.2, respectively. Compartmental model-derived *DV* values agreed well with *DV*s estimated by Logan graphical analysis (table 1). Apart from *DV*, the influx rate constant K_1 was also markedly increased after administration of different inhibitor doses (table 1).

Sigmoidal Hill curves were fitted to *DV* values plotted either against different inhibitor doses (Fig. 2a) or concentration levels of inhibitor in plasma (Fig. 2b). For tariquidar, ED_{50}=3.0±0.2 mg/kg, DV_{max}=11.9±0.5 ml·ml^{-1} and n=3.0±0.6 were estimated. The fitted parameters for elacridar were ED_{50}=1.2±0.1 mg/kg, DV_{max}=11.4±0.7 ml·ml^{-1} and n=5.2±2.8. For the concentration-response curves, estimated EC_{50} values were 545.0±29.9 ng/ml for tariquidar and 114.5±22.2 ng/ml for elacridar (Fig. 2b). As for *DV*, K_1 and k_3 values also showed sigmoidal dose-response relationships, whereas k_2 values stayed rather constant over increasing inhibitor doses (data not shown). For tariquidar, mean plasma and brain concentration values measured at 180 min after drug administration at a dose of 15 mg/kg (n=4) were 4003±390 ng/ml and 6453±3596 ng/ml, respectively (brain-to-plasma ratio: 1.7±0.9). These values were different from previously reported values [3], which might be related to the fact that a different rat strain was used in this study. For the 3 mg/kg dose mean plasma and brain concentration values (n=6) of tariquidar at 210 min after drug administration were 503±139 and 457±37 ng/ml, respectively (brain-to-plasma ratio: 1.0±0.3). For elacridar given at a dose of 5 mg/kg (n=5), these values were 316±61 ng/ml and 5186±1415 ng/ml (brain-to-plasma ratio: 16.8±5.8).

TACs for the 240 min VPM PET scans during which tariquidar (15 mg/kg) or elacridar (5 mg/kg) were administered (each at 60 min after radiotracer injection) are shown in Fig. 3. Brain activity started to rise in immediate response to inhibitor administration, with peak uptake reached at 30±5 min after inhibitor injection. After peak uptake, the TACs following tariquidar administration declined more rapidly than the TACs following elacridar administration.

In 6 animals, metabolism of VPM was studied. The percentages of unchanged VPM and its lipophilic [^{11}C]metabolites were 77±8, 63±10, 57±9, 45±5 and 46±7% at 10, 20, 30, 40 and 60 min after injection of VPM. In inhibitor-treated animals the percentages of unchanged VPM and its lipophilic [^{11}C]metabolites at 20 min after radiotracer injection were 61±9% for tariquidar (mean value for the 6 employed doses) and 64±14% for elacridar (mean value for the 5 employed doses), which was similar to the value in untreated animals (63±10%). At 60 min after radiotracer injection these values were 45±7% for tariquidar-treated and 45±5% for elacridar-treated animals (untreated animals: 46±7%). Similarly, the protein bound percentage of VPM in plasma was comparable before and after inhibitor administration (78.2±4.2%, 80.5±3.3% and 77.3±1.3% for baseline, tariquidar and elacridar samples, respectively; $p>0.4$).

For the paired scans before and after tariquidar (3 mg/kg) administration, 6 different brain ROIs were outlined on MR images that were co-registered with the PET images. Fig. 4 shows example MR, PET and co-registered images with outlined ROIs. Model outcome parameters of paired scans are summarised in table 2 and *DV*s of both scans are displayed in Fig. 5. In baseline experiments, *DV* values for ROIs ranged from 1.28 for hippocampus to 2.38 for frontal motor cortex. The *DV*s in all brain regions were statistically different to each other, except for cerebellum *vs.* frontal motor cortex and entorhinal cortex, frontal motor cortex *vs.* entorhinal cortex, corpus striatum *vs.* hippocampus and thalamus, and hippocampus *vs.* thalamus. Following tariquidar administration, *DV* ($p<0.001$) and K_1, k_3 and k_4 values ($p<0.02$), but not k_2 values ($p>0.34$), were significantly increased as compared to scan 1 in all ROIs. *DV* values for the selected ROIs in scan 2 ranged from 6.14 for cerebellum to 9.64 for thalamus (Fig. 5). Mean *DV* increases were 2.8±0.7, 3.1±1.1, 5.9±1.1, 3.0±1.4, 6.4±0.9, and 7.1±1.1 of baseline *DV* for cerebellum, frontal motor cortex, corpus striatum, entorhinal cortex, hippocampus, and thalamus, respectively. The *DV*s in all brain regions for scan 2 were statistically different to each other, except for cerebellum *vs.* entorhinal cortex, hippocampus *vs.* frontal motor cortex and corpus striatum, and corpus striatum *vs.* thalamus.

Discussion

The aim of this study was to identify a suitable P-gp inhibitor that can be used to enhance brain uptake of VPM and thereby improve the mapping of regional differences in cerebral P-gp function and expression. We performed a detailed dose-response assessment of tariquidar and the structurally related P-gp inhibitor elacridar. Moreover, we performed paired PET scans in rats before and after administration of a tariquidar dose that does not completely inhibit cerebral P-gp function. This paradigm allowed us to quantify regional differences in P-gp function demonstrated by tariquidar-mediated changes in VPM brain uptake.

The third-generation P-gp inhibitors tariquidar and elacridar are among the most potent and selective P-gp inhibitors known to date. Unlike first-generation P-gp inhibitors, such as verapamil or cyclosporine A, they are non-competitive inhibitors and not substrates of P-gp [16, 17]. *In vitro*, tariquidar and elacridar inhibited P-gp mediated transport of the P-gp substrate [^{3}H]paclitaxel in a P-gp overexpressing cell line (CH^{r}B30) with inhibition constants (K_i) of 25 and 109 nM, respectively [16]. Preclinical studies have shown that

tariquidar and elacridar potently inhibit P-gp function at the BBB as reflected by increased brain uptake of P-gp substrates, without displaying cytochrome P450 mediated pharmacokinetic interactions [3, 18, 19]. Tariquidar and elacridar also inhibit breast cancer resistance protein (BCRP, ABCG2), another ABC-type transporter expressed at the BBB, with half-maximum inhibitory concentrations (IC_{50}) of 916 and 250 nM, respectively (determined for inhibition of mitoxantrone transport in a BCRP-overexpressing cell line) [20]. However, unlike first- and second-generation P-gp inhibitors they do not inhibit multidrug resistance-associated proteins (MRPs), such as MRP1 [1].

We previously performed a pilot small animal PET study in rats, which were imaged with VPM before and after administration of 15 mg/kg tariquidar and showed an approximately 12-fold *DV* increase following tariquidar [3]. Our current data are in line with other previous preclinical data [3, 18, 19] as they give evidence that tariquidar and elacridar markedly increase brain distribution of the P-gp substrate VPM. However, unlike previous studies we performed a detailed dose-response assessment for both inhibitors, as this information is a prerequisite for using these compounds in preclinical and clinical PET experiments. Here we show that elacridar (ED_{50}=1.20±0.14 mg/kg) is about 3 times more potent than tariquidar (ED_{50}=3.00±0.19 mg/kg) in increasing brain distribution of VPM. At maximum doses both inhibitors increased *DV*s to a similar extent. Our findings are in reasonable agreement with previous data from Choo *et al.* who reported ED_{50} values of 5.7 mg/kg for tariquidar and 2.4 mg/kg for elacridar for enhancing the brain-to-plasma ratios of the P-gp substrate loperamide in mice [18]. The higher *in vivo* potency of elacridar might be related to better access of elacridar to its target structures in the BBB, as reflected by about 10-fold higher brain-to-plasma ratios of elacridar as compared to tariquidar. In our setting, both tariquidar and elacridar appeared to exert no effect on metabolism and plasma protein binding of VPM, which is important as changes in these two parameters might confound the effect of P-gp inhibition on brain uptake of activity.

In an additional group of animals we administered the inhibitors during rather than before the VPM PET scan. This set-up offers the advantage that the dynamics of the entire P-gp inhibition process can be monitored. We have shown before, both in rats and in humans, that VPM metabolism is quite slow, resulting in significant amounts of unchanged parent still present in plasma at 60 min after tracer injection, and that activity reaches transient equilibrium both in plasma and brain at 60 min after VPM injection [3, 9]. Hence, the activity influx seen in Fig. 3 following inhibitor administration was presumably caused by inhibitorinduced P-gp blockade which facilitated brain entry of circulating activity by passive diffusion. Interestingly, the brain TACs indicated that both inhibitors were fast acting (maximum effect at 30 min after inhibitor administration) and that the effect of tariquidar, as opposed to that of elacridar, was at least partially reversible, as reflected by the more rapid decline of the TACs following peak uptake after tariquidar administration.

We previously conducted a pilot study in healthy volunteers in which we assessed the effect of 2 mg/kg tariquidar on VPM brain distribution [9]. Interestingly, comparable plasma concentrations of tariquidar led to marked species differences in enhancement of VPM brain uptake. In rats, the ED_{50} of tariquidar in plasma (545.0±29.9 ng/ml) corresponded to an approximately 4-fold increase of brain *DV*s (Fig. 2), whereas in humans a tariquidar plasma concentration of 490±203 ng/ml at the time of the PET scan led to an only 1.24-fold increase of brain *DV*s. Species differences with respect to the P-gp system have been described before. Cutler *et al.* found that about 10 times higher plasma concentration levels of elacridar are needed in guinea pigs as compared to rats and mice to achieve the same degree of brain distribution increases of an undisclosed P-gp substrate in the three species [19]. Syvänen and co-workers reported that 3 different PET radiotracers which are P-gp substrates (i.e. racemic [^{11}C]verapamil, [^{11}C]GR205171 and [^{18}F]altanserin) had several times lower

brain-to-plasma ratios of activity in rats as compared to monkeys or humans and also exhibited greater responses in terms of brain distribution increases in rats as compared to monkeys following a cyclosporine A challenge [21]. For instance, for [^{11}C]verapamil the brain-to-plasma ratio of activity was 1.13 in rats and 4.61 in monkeys; brain-to-plasma ratios were increased 5.8-fold in rats and 3.6-fold in monkeys at comparable cyclosporine A plasma concentration levels [21]. When comparing our own data acquired in rats and humans we cannot confirm the pronounced differences in brain-to-plasma ratios of activity in VPM baseline scans (i.e. before P-gp inhibition) as reported by Syvänen for rats and monkeys. In fact, mean *DV* values of VPM in whole brain, which can be considered a very similar measure to the brain-to-plasma ratio, were about 2 times higher in rats as compared to humans (1.28±0.17 *versus* 0.65±0.13 [9]. These differences between rats and humans can most likely be explained by species differences in VPM metabolism. Rats had an approximately 2 times higher percentage of polar [^{11}C]metabolites of VPM in plasma (54% *versus* 26% [9] for rats and humans, respectively, both at 40 min after radiotracer injection). As these polar metabolites have been shown to be taken up into brain tissue [14], presumably independent of P-gp function, a higher contribution of polar [^{11}C]metabolites to the brain PET signal in rats as compared to humans might explain the higher baseline *DV* values in rats. On the other hand, our data are in good agreement with the data from Syvänen [21] in that we also observed pronounced species differences in terms of *DV* increases following administration of a P-gp inhibitor. In fact, the differences between rats and humans seen in our study for tariquidar were even greater than the differences reported by Syvänen for cyclosporine A in rats and monkeys. Possible explanations for this finding could be species differences in the pharmacokinetic properties of tariquidar (e.g. plasma protein binding, brain distribution) or species differences in cerebral P-gp function and/or expression. In addition, it cannot be ruled out that isoflurane anaesthesia might have had an effect on the PET results acquired in rats and thereby biased the comparison between rat and human data. However, given the magnitude of differences in tariquidar-induced P-gp inhibition seen between rats and humans it seems unlikely that these differences were only caused by anaesthesia effects.

We performed paired small animal PET scans in rats before and after administration of tariquidar at the ED_{50} in order to study regional differences in tariquidar-induced modulation of VPM brain distribution. We selected tariquidar as the preferred inhibitor for this study paradigm as the dose-response curve was less steep as compared to elacridar (Fig. 2), which will cause less inter-subject variability in *DV* increases when inhibitor is given at the ED_{50}. A second reason was the fact that pharmaceutical-grade tariquidar was available for clinical use, whereas elacridar was not. According to the dose-response assessment shown in Fig. 2, doses above 6 mg/kg of tariquidar lead to complete inhibition of P-gp, resulting in brain uptake of VPM driven by passive diffusion only. In addition, brain uptake of VPM at high inhibitor doses might become susceptible to changes in cerebral blood flow, which will blunt possible regional differences in P-gp function [22]. The ED_{50} of tariquidar (3 mg/kg) seemed to be a good compromise between sufficient activity signal for PET imaging in selected brain areas and only partial inhibition of P-gp.

We selected 6 brain ROIs for data analysis. These regions were chosen as they are rather large, therefore partial volume effects should be low. In the baseline experiments (i.e. before inhibition), *DV* values of VPM in ROIs were rather low (table 2), which suggested that VPM is efficiently kept out of brain by P-gp mediated efflux. Moreover, a considerable part of the baseline brain PET signal might have been due to polar [^{11}C]metabolites of VPM, whose brain retention is independent of regional differences in P-gp function and expression. However, there were clear-cut differences between the studied brain regions in modulation of VPM brain distribution following tariquidar administration, which we hypothesise to reflect regional differences in P-gp function and expression. Presumably, a

greater response to tariquidar treatment, as we saw in corpus striatum, hippocampus and thalamus, reflected lower functionality and density of P-gp, whereas a smaller response (e.g. cerebellum, cortical regions) was indicative of higher P-gp functionality and density. It cannot be ruled out, however, that at least part of the regional differences in VPM brain uptake following tariquidar administration were related to regional differences in cerebral blood flow rather than differences in P-gp function or expression. However, given the magnitude of the differences seen in individual brain ROIs it seems unlikely that these differences were only related to cerebral blood flow. Clearly, further studies are needed in order to assess whether VPM uptake is flow dependent in rat brain after administration of tariquidar at a dose of 3 mg/kg.

In order to validate our results, data about the regional distribution pattern of P-gp in rat brain would be needed. Only limited information for P-gp expression in brain regions examined in our study is available at present [23, 24]. A previous animal imaging study found some evidence for a non-uniform distribution of P-gp in rat brain [25]. Laćan *et al.* quantified P-gp expression by Western blot analysis and found 2 times higher P-gp levels in cerebellum as compared to other brain regions (hippocampus, frontal cortex) of rats [25]. This is in line with a study by van Vliet *et al.* [23] in which P-gp expression was also investigated by Western blot analysis in cerebellum, septal and temporal hippocampus, parahippocampal cortex, and bulbus olfactorius. Although no quantitative analysis was performed, the data indicate highest P-gp expression in cerebellum. Volk *et al.* [24] quantified P-gp expression by optical density measurements of immunohistochemically stained brain sections. While no differences were detected in optical density, the P-gp-labelled area was distinctly higher in piriform cortex as compared to hippocampal subregions. In line with these previous results, in our study DV in scan 2 was lowest in cerebellum and entorhinal cortex (which is closely interconnected to piriform cortex) and significantly lower as compared to DVs from hippocampus and frontal motor cortex. Notably, in contrast to DV in scan 2, baseline DV values in cerebellum were the second highest, which suggests that baseline DV values are blunted by radiolabelled metabolites of VPM which are taken up into brain independent of P-gp function. Interestingly, in a previous human PET study in which differences in tariquidar-induced P-gp modulation were investigated in 42 brain ROIs [26], a similar rank order of regional DV increases was seen as in the present study, with smaller DV increases in cortical regions and greater DV increases in corpus striatum and putamen, which suggests that possible regional differences in P-gp function might be conserved between species.

Conclusion

We performed a dose-response assessment of the two third-generation P-gp inhibitors tariquidar and elacridar and quantified cerebral P-gp activity in rat brain using PET and the radiolabelled P-gp substrate VPM. Both inhibitors were fast acting and able to increase VPM brain distribution up to 11-fold over baseline at maximum effective doses. Elacridar was about 3 times more potent than tariquidar in increasing VPM brain distribution. Tariquidar administered at the ED_{50} (3 mg/kg) was chosen as preferred inhibitor for a paired scan paradigm to study regional differences in cerebral P-gp function and expression. DVs after P-gp inhibition were smallest in cerebellum and greatest in thalamus, which pointed to lower P-gp function and expression in thalamus as compared to cerebellum. Further studies are needed to assess the possible influence of cerebral blood flow on VPM brain uptake. Additionally, regional differences in tariquidar-induced modulation of VPM brain uptake have to be further related to regional P-gp expression levels in rat brain determined by independent methods.

Acknowledgments

The research leading to these results has received funding from the European Community's Seventh Framework Programme (FP7/2007-2013) under grant agreement number 201380 ("Euripides") and from the Austrian Science Fund (FWF) project "Transmembrane Transporters in Health and Disease" (SFB F35). The authors thank Thomas Filip and Maria Zsebedics (Seibersdorf Laboratories GmbH) for their skilful help with laboratory animal handling and the staff of the radiochemistry laboratory (Seibersdorf Laboratories GmbH) for their continuous support. Thomas Flanitzer is gratefully acknowledged for help with the data analysis and Ronald Boellaard (VU University Medical Center, Amsterdam, The Netherlands) for advice on compartment modelling issues.

References

1. Löscher W, Potschka H. Role of drug efflux transporters in the brain for drug disposition and treatment of brain diseases. Prog Neurobiol. 2005; 76(1):22–76. [PubMed: 16011870]
2. Lubberink M, Luurtsema G, van Berckel BN, Boellaard R, Toornvliet R, Windhorst AD, et al. Evaluation of tracer kinetic models for quantification of P-glycoprotein function using (R)-[(11)C]verapamil and PET. J Cereb Blood Flow Metab. 2007; 27(2):424–33. [PubMed: 16757979]
3. Bankstahl JP, Kuntner C, Abrahim A, Karch R, Stanek J, Wanek T, et al. Tariquidar-induced P-glycoprotein inhibition at the rat blood-brain barrier studied with (R)-11C-verapamil and PET. J Nucl Med. 2008; 49(8):1328–35. [PubMed: 18632828]
4. Bart J, Willemsen AT, Groen HJ, van der Graaf WT, Wegman TD, Vaalburg W, et al. Quantitative assessment of P-glycoprotein function in the rat blood-brain barrier by distribution volume of [11C]verapamil measured with PET. Neuroimage. 2003; 20(3):1775–82. [PubMed: 14642487]
5. Bartels AL, van Berckel BN, Lubberink M, Luurtsema G, Lammertsma AA, Leenders KL. Blood-brain barrier P-glycoprotein function is not impaired in early Parkinson's disease. Parkinsonism Relat Disord. 2008; 14(6):505–8. [PubMed: 18325822]
6. Langer O, Bauer M, Hammers A, Karch R, Pataraia E, Koepp MJ, et al. Pharmacoresistance in epilepsy: a pilot PET study with the P-glycoprotein substrate R-[11C]verapamil. Epilepsia. 2007; 48(9):1774–84. [PubMed: 17484754]
7. Lee YJ, Maeda J, Kusuhara H, Okauchi T, Inaji M, Nagai Y, et al. In vivo evaluation of P-glycoprotein function at the blood-brain barrier in nonhuman primates using [11C]verapamil. J Pharmacol Exp Ther. 2006; 316(2):647–53. [PubMed: 16293715]
8. Sasongko L, Link JM, Muzi M, Mankoff DA, Yang X, Collier AC, et al. Imaging P-glycoprotein transport activity at the human blood-brain barrier with positron emission tomography. Clin Pharmacol Ther. 2005; 77(6):503–14. [PubMed: 15961982]
9. Wagner CC, Bauer M, Karch R, Feurstein T, Kopp S, Chiba P, et al. A pilot study to assess the efficacy of tariquidar to inhibit P-glycoprotein at the human blood-brain barrier with (R)–11C-verapamil and PET. J Nucl Med. 2009 in press.
10. Brunner M, Langer O, Sunder-Plassmann R, Dobrozemsky G, Müller U, Wadsak W, et al. Influence of functional haplotypes in the drug transporter gene ABCB1 on central nervous system drug distribution in humans. Clin Pharmacol Ther. 2005; 78(2):182–90. [PubMed: 16084852]
11. Tai YC, Ruangma A, Rowland D, Siegel S, Newport DF, Chow PL, et al. Performance evaluation of the microPET focus: a third-generation microPET scanner dedicated to animal imaging. J Nucl Med. 2005; 46(3):455–63. [PubMed: 15750159]
12. Pauli-Magnus C, von Richter O, Burk O, Ziegler A, Mettang T, Eichelbaum M, et al. Characterization of the major metabolites of verapamil as substrates and inhibitors of P-glycoprotein. J Pharmacol Exp Ther. 2000; 293(2):376–82. [PubMed: 10773005]
13. Abrahim A, Luurtsema G, Bauer M, Karch R, Lubberink M, Pataraia E, et al. Peripheral metabolism of (R)-[(11)C]verapamil in epilepsy patients. Eur J Nucl Med Mol Imaging. 2008; 35:116–23. [PubMed: 17846766]
14. Luurtsema G, Molthoff CF, Schuit RC, Windhorst AD, Lammertsma AA, Franssen EJ. Evaluation of (R)-[11C]verapamil as PET tracer of P-glycoprotein function in the blood-brain barrier: kinetics and metabolism in the rat. Nucl Med Biol. 2005; 32(1):87–93. [PubMed: 15691665]
15. Loening AM, Gambhir SS. AMIDE: a free software tool for multimodality medical image analysis. Mol Imaging. 2003; 2(3):131–7. [PubMed: 14649056]

16. Martin C, Berridge G, Mistry P, Higgins C, Charlton P, Callaghan R. The molecular interaction of the high affinity reversal agent XR9576 with P-glycoprotein. Br J Pharmacol. 1999; 128(2):403–11. [PubMed: 10510451]

17. Polli JW, Wring SA, Humphreys JE, Huang L, Morgan JB, Webster LO, et al. Rational use of in vitro P-glycoprotein assays in drug discovery. J Pharmacol Exp Ther. 2001; 299(2):620–8. [PubMed: 11602674]

18. Choo EF, Kurnik D, Muszkat M, Ohkubo T, Shay SD, Higginbotham JN, et al. Differential in vivo sensitivity to inhibition of P-glycoprotein located in lymphocytes, testes, and the blood-brain barrier. J Pharmacol Exp Ther. 2006; 317(3):1012–8. [PubMed: 16537797]

19. Cutler L, Howes C, Deeks NJ, Buck TL, Jeffrey P. Development of a P-glycoprotein knockout model in rodents to define species differences in its functional effect at the blood-brain barrier. J Pharm Sci. 2006; 95(9):1944–53. [PubMed: 16850390]

20. Kuhnle M, Egger M, Muller C, Mahringer A, Bernhardt G, Fricker G, et al. Potent and selective inhibitors of breast cancer resistance protein (ABCG2) derived from the p-glycoprotein (ABCB1) modulator tariquidar. J Med Chem. 2009; 52(4):1190–7. [PubMed: 19170519]

21. Syvänen S, Lindhe O, Palner M, Kornum BR, Rahman O, Langstrom B, et al. Species differences in blood-brain barrier transport of three PET radioligands with emphasis on P-glycoprotein transport. Drug Metab Dispos. 2009; 37(3):635–43. [PubMed: 19047468]

22. Liow JS, Kreisl W, Zoghbi SS, Lazarova N, Seneca N, Gladding RL, et al. P-Glycoprotein Function at the Blood-Brain Barrier Imaged Using 11C-N-Desmethyl-Loperamide in Monkeys. J Nucl Med. 2009; 50(1):108–15. [PubMed: 19091890]

23. van Vliet EA, van Schaik R, Edelbroek PM, Voskuyl RA, Redeker S, Aronica E, et al. Region-specific overexpression of P-glycoprotein at the blood-brain barrier affects brain uptake of phenytoin in epileptic rats. J Pharmacol Exp Ther. 2007; 322(1):141–7. [PubMed: 17392402]

24. Volk HA, Potschka H, Loscher W. Increased expression of the multidrug transporter P-glycoprotein in limbic brain regions after amygdala-kindled seizures in rats. Epilepsy Res. 2004; 58(1):67–79. [PubMed: 15066676]

25. Laćan G, Plenevaux A, Rubins DJ, Way BM, Defraiteur C, Lemaire C, et al. Cyclosporine, a P-glycoprotein modulator, increases [18F]MPPF uptake in rat brain and peripheral tissues: microPET and ex vivo studies. Eur J Nucl Med Mol Imaging. 2008; 35(12):2256–66. [PubMed: 18604533]

26. Bauer M, Wagner CC, Kletter K, Zeitlinger M, Müller M, Langer O. Regional differences in P-glycoprotein function at the human blood-brain barrier [symposium abstract]. J Nucl Med. 2009; 50(Supplement 2):223P.

27. Paxinos, G.; Watson, C. The Rat Brain in Stereotaxic Coordinates. 6th ed. Academic Press; London: 2007.

Europe PMC Funders Author Manuscripts

Europe PMC Funders Author Manuscripts

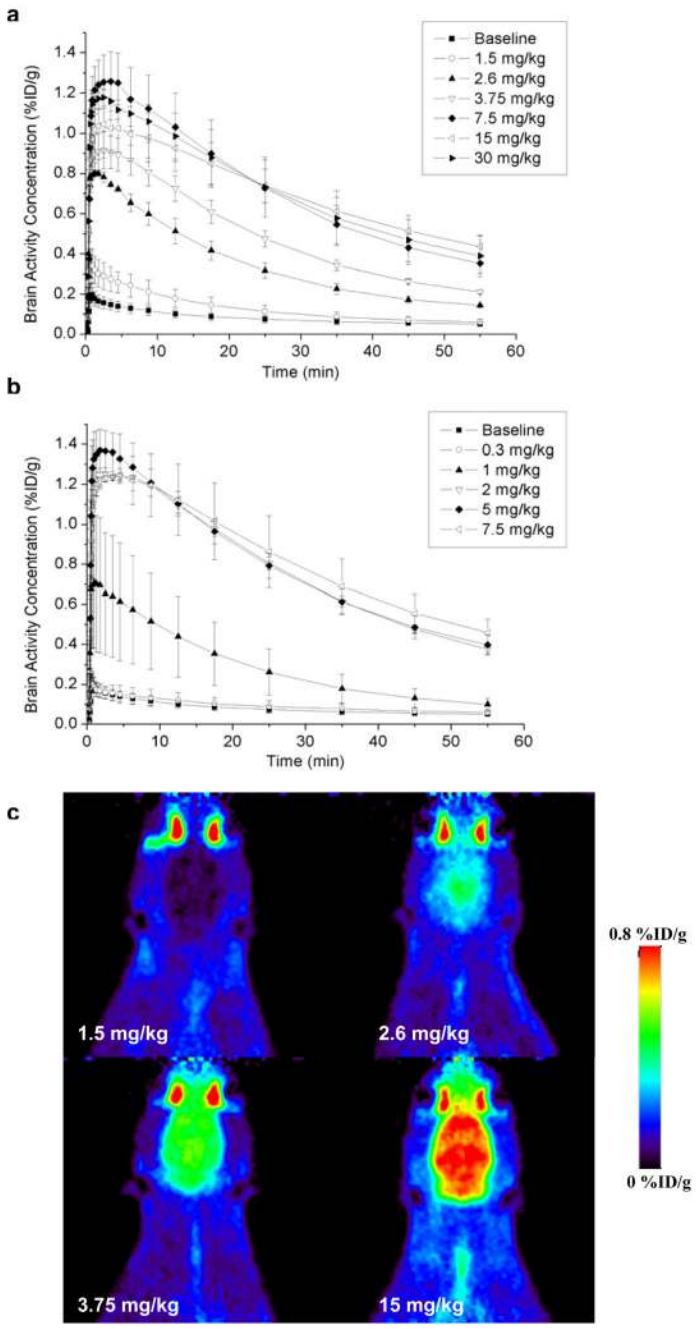

Fig. 1.

TACs (mean %ID/g±SD) of VPM in whole brain beginning 120 min after administration of (**a**) 1.5, 2.6, 3.75, 7.5, 15 and 30 mg/kg of tariquidar (n=2 per dose) and (**b**) 0.3, 1, 2, 5, and 7.5 mg/kg of elacridar (n=2 per dose, except for 1 and 5 mg/kg (n=3)), respectively. In addition, horizontal PET summation images after administration of 1.5 (upper left), 2.6 (upper right), 3.75 (lower left) and 15 mg/kg (lower right) of tariquidar are shown (**c**)

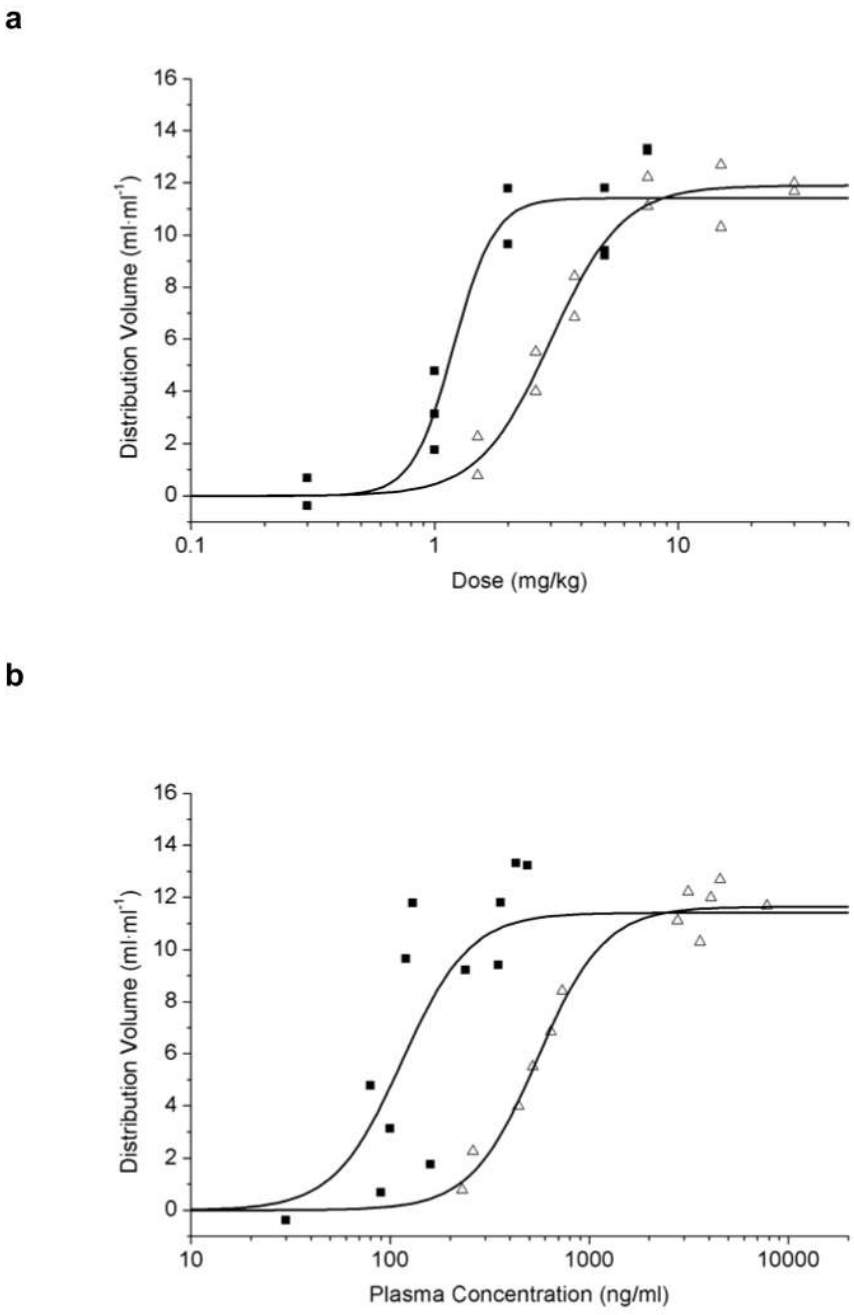

Fig. 2.

*DV*s of VPM in whole brain after administration of tariquidar (open triangles) or elacridar (filled squares) plotted against inhibitor dose (mg/kg) (**a**) or inhibitor plasma concentration (ng/ml) (**b**). Note that x-axes are in a logarithmic scale. Plasma concentrations were determined in arterial blood samples collected at the end of the PET scan (i.e. at 180 min after inhibitor administration) by LC/MS analysis. Sigmoidal Hill curves were fitted to the data and gave estimated ED_{50} values of 3.0±0.2 and 1.2±0.1 mg/kg and EC_{50} values of 545.0±29.9 and 114.5±22.2 ng/ml for tariquidar and elacridar, respectively

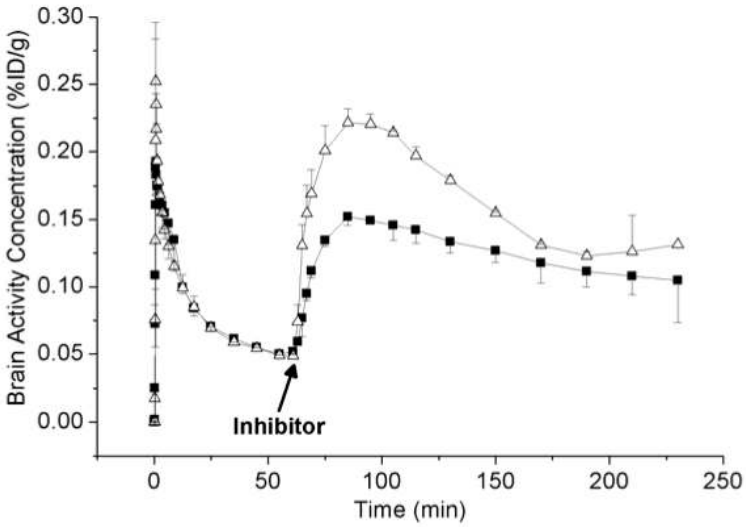

Fig. 3.

TACs (mean %ID/g±SD) of VPM in whole brain for the 240-min scans, during which tariquidar (15 mg/kg, open triangles) or elacridar (5 mg/kg, filled squares) was administered (each at 60 min after radiotracer injection). The time point of inhibitor administration is indicated by an arrow

Europe PMC Funders Author Manuscripts

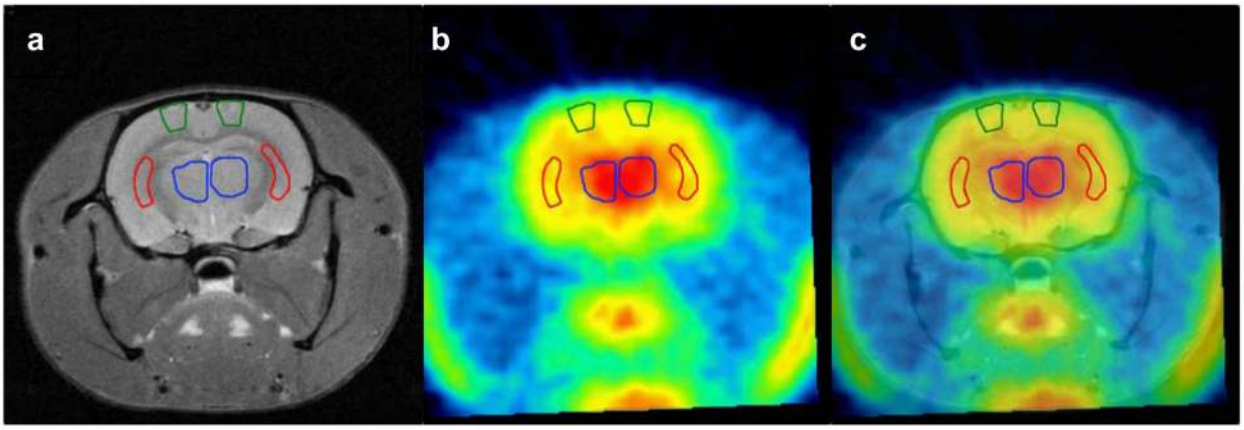

Fig. 4.

Representative coronal small animal MR (**a**), PET summation (0-60 min) (**b**) and co-registered images (**c**) of a rat (−2.0 mm relative to bregma, according to [27]) after administration of tariquidar (3 mg/kg). The following ROIs are shown: frontal motor cortex (green), corpus striatum (red) and thalamus (blue)

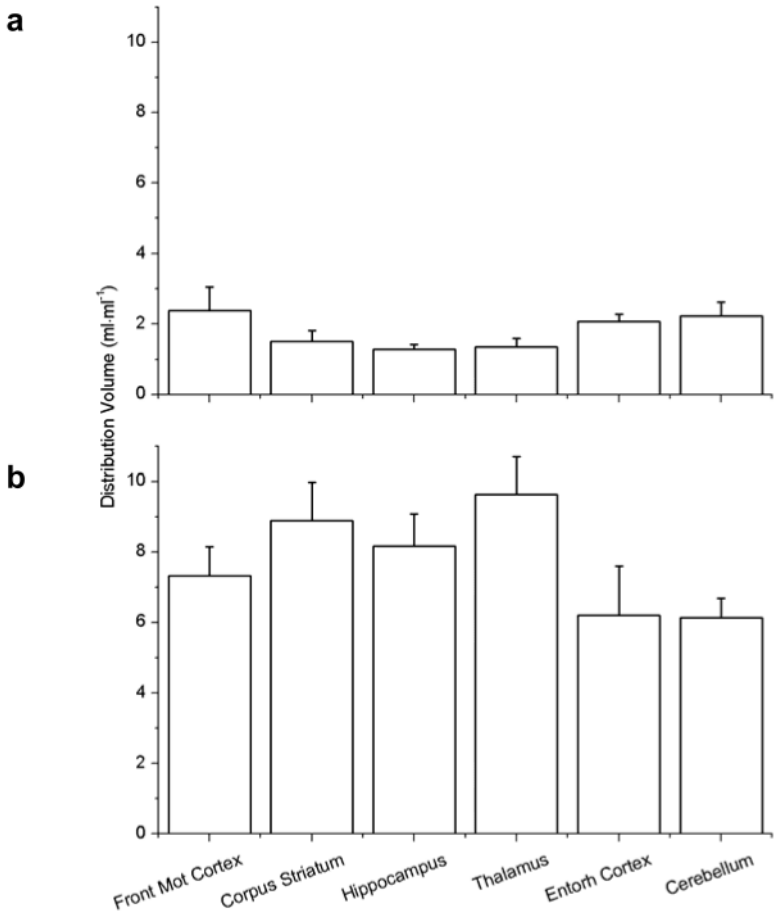

Fig. 5.

Mean (±SD) *DV*s (*n*=6) for the paired VPM PET scans in the defined brain regions before (**a**) and after (**b**) administration of 3 mg/kg tariquidar (Front Mot Cortex: frontal motor cortex; Entorh Cortex: entorhinal cortex). Statistically different brain regions are described in the Results section.

Europe PMC Funders Author Manuscripts

Table 1

Outcome parameters (whole brain) of 2T4K model for baseline scans and scans after administration of different tariquidar or elacridar doses

Baseline	**K_1 ($ml \cdot ml^{-1} \cdot min^{-1}$)**	**k_2 (min^{-1})**	**k_3 (min^{-1})**	**k_4 (min^{-1})**	**DV ($ml \cdot ml^{-1}$)**	***DV* (Logan) ($ml \cdot ml^{-1}$)**
	0.16±0.05 (20)	0.36±0.07 (43)	0.11±0.06 (46)	0.05±0.02 (24)	1.27±0.15 (5)	1.20±0.14 (4)
Tariquidar	K_1 ($ml \cdot ml^{-1} \cdot min^{-1}$)	k_2 (min^{-1})	k_3 (min^{-1})	k_4 (min^{-1})	*DV* ($ml \cdot ml^{-1}$)	*DV* (Logan) ($ml \cdot ml^{-1}$)
1.5 mg/kg	0.38±0.17 (11.4)	0.26±0.07 (29.2)	0.09±0.03 (61.2)	0.11±0.08 (20.6)	2.80±1.05 (6.3)	2.70±0.91 (1.7)
2.6 mg/kg	0.78±0.01 (15.6)	0.36±0.09 (34.5)	0.16±0.04 (40.6)	0.10±0.01 (15.9)	6.03±1.07 (2.7)	5.90±1.05 (1.7)
3.75 mg/kg	0.81±0.16 (13.9)	0.18±0.05 (50.3)	0.20±0.02 (101.3)	0.22±0.07 (51.4)	8.92±1.11 (2.3)	8.80±1.06 (0.9)
7.5 mg/kg	1.27±0.24 (17.4)	0.31±0.12 (82.5)	0.37±0.10 (97.3)	0.18±0.01 (23.9)	12.93±0.79 (1.7)	12.66±0.77 (0.9)
15 mg/kg	1.02±0.02 (15.0)	0.43±0.16 (50.3)	0.48±0.04 (39.2)	0.12±0.02 (20.4)	12.72±1.83 (1.8)	12.35±1.79 (1.4)
30 mg/kg	1.22±0.23 (11.2)	0.30±0.04 (54.6)	0.38±0.18 (59.4)	0.17±0.09 (19.8)	13.11±0.22 (2.1)	12.76±0.04 (0.7)
Elacridar	K_1 ($ml \cdot ml^{-1} \cdot min^{-1}$)	k_2 (min^{-1})	k_3 (min^{-1})	k_4 (min^{-1})	*DV* ($ml \cdot ml^{-1}$)	*DV* (Logan) ($ml \cdot ml^{-1}$)
0.3 mg/kg	0.13±0.10 (16.5)	0.29±0.06 (36.5)	0.14±0.02 (41.4)	0.07±0.01 (16.7)	1.28±0.54 (3.1)	1.22±0.51 (2.9)
1 mg/kg	0.57±0.19 (18.1)	0.33±0.10 (78.9)	0.29±0.11 (93.2)	0.19±0.06 (33.3)	4.49±1.51 (2.9)	4.47±1.51 (0.9)
2 mg/kg	0.92±0.16 (7.2)	0.18±0.06 (42.2)	0.29±0.09 (68.5)	0.22±0.03 (21.1)	12.00±1.49 (2.4)	11.72±1.47 (0.6)
5 mg/kg	0.93±0.26 (17.0)	0.22±0.06 (58.8)	0.28±0.05 (79.7)	0.16±0.01 (35.4)	11.40±1.45 (3.8)	11.16±1.44 (1.1)
7.5 mg/kg	0.98±0.08 (6.4)	0.15±0.02 (43.5)	0.25±0.07 (55.4)	0.22±0.04 (30.3)	14.55±0.06 (2.6)	14.20±0.13 (0.4)

Outcome parameters are given as mean±SD averaged over all animals per dose group. The value in parentheses represents the precision of parameter estimates (expressed as their coefficient of variation in percent), averaged over all animals per dose group.

Table 2

Outcome parameters of 2T4K model for paired VPM PET scans before and after 3 mg/kg tariquidar in different brain regions

Brain region Before inhibition	K_1 *(ml·ml^{-1}·min^{-1})*	k_2 *(min^{-1})*	k_3 *(min^{-1})*	k_4 *(min^{-1})*	DV *(ml·ml^{-1})*	DV *(Logan)* *(ml·ml^{-1})*
Cerebellum	0.19±0.04 (12.8)	0.28±0.06 (30.1)	0.11±0.05 (35.9)	0.05±0.02 (19.3)	2.23±0.40 (5.2)	1.99±0.37 (3.7)
Frontal motor cortex	0.17±0.07 (12.3)	0.22±0.09 (33.1)	0.12±0.07 (41.1)	0.05±0.02 (24.3	2.38±0.67 (6.0)	2.12±0.69 (3.0)
Corpus striatum	0.11±0.03 (15.5)	0.26±0.07 (39.5)	0.11±0.05 (45.2)	0.04±0.02 (25.0)	1.50±0.31 (7.8)	1.31±0.29 (4.4)
Entorhinal cortex	0.20±0.04 (18.5)	0.32±0.10 (38.2)	0.11±0.04 (46.1)	0.05±0.02 (26.3)	2.08±0.20 (6.4)	1.88±0.19 (3.5)
Hippocampus	0.11±0.03 (17.7)	0.30±0.07 (44.0)	0.12±0.04 (49.6)	0.05±0.01 (26.3)	1.28±0.15 (6.8)	1.17±0.19 (4.2)
Thalamus	0.11±0.01 (18.7)	0.26±0.08 (36.8)	0.10±0.04 (55.2)	0.05±0.01 (35.2)	1.35±0.25 (7.9)	1.21±0.19 (4.5)

Brain region After inhibition	K_1 *(ml·ml^{-1}·min^{-1})*	k_2 *(min^{-1})*	k_3 *(min^{-1})*	k_4 *(min^{-1})*	DV *(ml·ml^{-1})*	***DV* (Logan)** **(ml·ml^{-1})**
Cerebellum	0.73±0.14 (11.7)	0.32±0.13 (46.6)	0.30±0.08 (75.2)	0.20±0.05 (26.4)	6.14±0.54 (2.9)	6.07±0.52 (0.9)
Frontal motor cortex	0.63±0.08 (9.5)	0.24±0.05 (49.6)	0.32±0.09 (68.7)	0.19±0.06 (23.8)	7.33±0.82 (1.7)	7.14±0.80 (0.9)
Corpus striatum	0.79±0.13 (10.5)	0.28±0.08 (46.6)	0.47±0.22 (53.4)	0.22±0.06 (23.1)	8.89±1.08 (2.7)	8.70±1.05 (0.6)
Entorhinal cortex	0.64±0.17 (12.9)	0.37±0.14 (57.5)	0.34±0.10 (68.9)	0.15±0.05 (22.5)	6.20±1.40 (3.4)	6.09±1.37 (1.1)
Hippocampus	0.75±0.11 (11.1)	0.32±0.08 (57.9)	0.43±0.09 (69.4)	0.18±0.05 (23.8)	8.17±0.91 (2.2)	8.01±0.88 (0.9)
Thalamus	0.93±0.12 (9.0)	0.33±0.18 (48.8)	0.47±0.11 (64.4)	0.23±0.06 (23.6)	9.64±1.06 (2.0)	9.45±1.03 (0.6)

Outcome parameters are given as mean±SD averaged over the 6 studied animals. The value in parentheses represents the precision of parameter estimates (expressed as their coefficient of variation in percent), averaged over the 6 studied animals.